Biogerontologia in Italia

Prof. P.Odetti, Università di Genova

La **Gerontologia** include ricercatori nel campo della
biologia,
medicina,
infermieristica,
riabilitazione,
farmacologia,
odontoiatria,
economia e scienze politiche,
psichiatria e psicologia,
sociologia e assistenza sociale,
architettura,
salute pubblica,
antropologia

La **Biogerontologia** è un una sotto-area essenziale:

- studia i cambiamenti fisici, mentali e sociali nelle persone che invecchiano
- indaga l'invecchiamento cellulare, d'organo e sistemico
- elabora approcci per modulare i processi molecolari alla base dei cambiamenti negativi legati all'invecchiamento e per contrastare le malattie età-dipendenti

Il termine **GERONTOLOGIA** è stato coniato da Elie Metchnikoff nel 1903.

James Birren (1940) inizia a organizzarla e nel 1945 viene fondata la Società Americana di Gerontologia.

Nel 1965 nasce il primo centro per lo studio dell'invecchiamento: Andrus Center of Gerontology (USC) dell'Università della California del Sud

Gli studi longitudinali di Baltimora sull'invecchiamento iniziano nel 1958, studiano i cambiamenti fisiologici in uomini sani di mezza età e in anziani che vivono in comunità, testando ogni due anni numerosi parametri fisiologici.

Da allora gli istituti di Gerontologia si sono moltiplicati anche in Europa
(***Insitute of Gerontology, Jönköping University, Svezia, 1975 -***
King's College London, UK, 1986 -
European center of Gerontology Malta, 1989 -
Danish Institute of Gerontology, Danimarca, 1989 -
Oxford University, UK, 2001 -
German Centre of Gerontology , Berlino, D, 2001)
ma non in Italia

E in Italia?

La SIGG ha sempre considerato la Bio-Gerontologia come necessaria, ma ospite, anche se, molti dei suoi ricercatori ne utilizzano gli strumenti

Molto lavoro prodotto da scienziati di base (biologi, patologi generali, biochimici, …)

Assenza di veri centri di Biogerontologia (master, corsi, congressi, …)

Abete
Barbagallo
Bergamini
Caruso
Ceda
Cellerino
Chiarpotto
Ferrara
Ferrucci
Fontana
Franceschi
Leosco
Longo
Mecocci
Moccheggiani
Odetti
Paolisso
Passarino
Rose
Rosenthal
Vendemiale
Zamboni

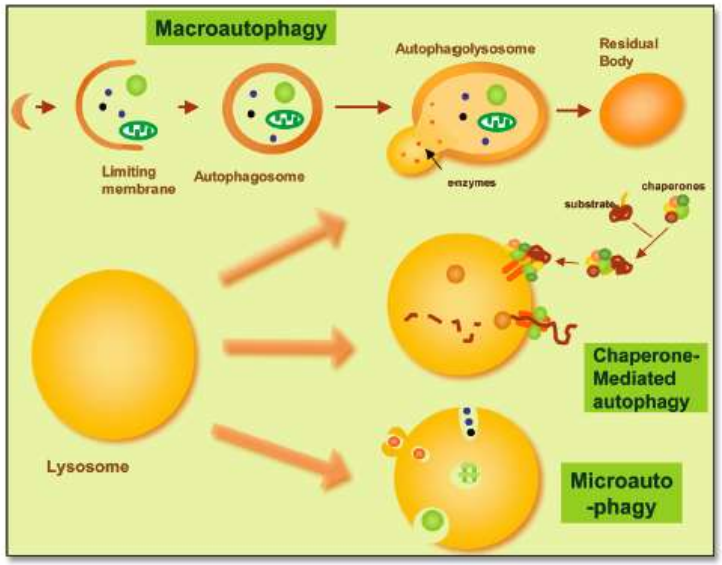

Figure 1. Schematic model of the types of autophagy in mammalian cells. Internalization of complete regions of cytosol first into autophagosomes that then fuse with lysosomes (macroautophagy), or directly by the lysosomal membrane (microautophagy) contrast with the selective uptake on a molecule-by-molecule basis of cytosolic proteins via chaperone-mediated autophagy.

E. Bergamini, PISA

Meccanismo anti-invecchiamento della restrizione calorica attraverso l'autofagia

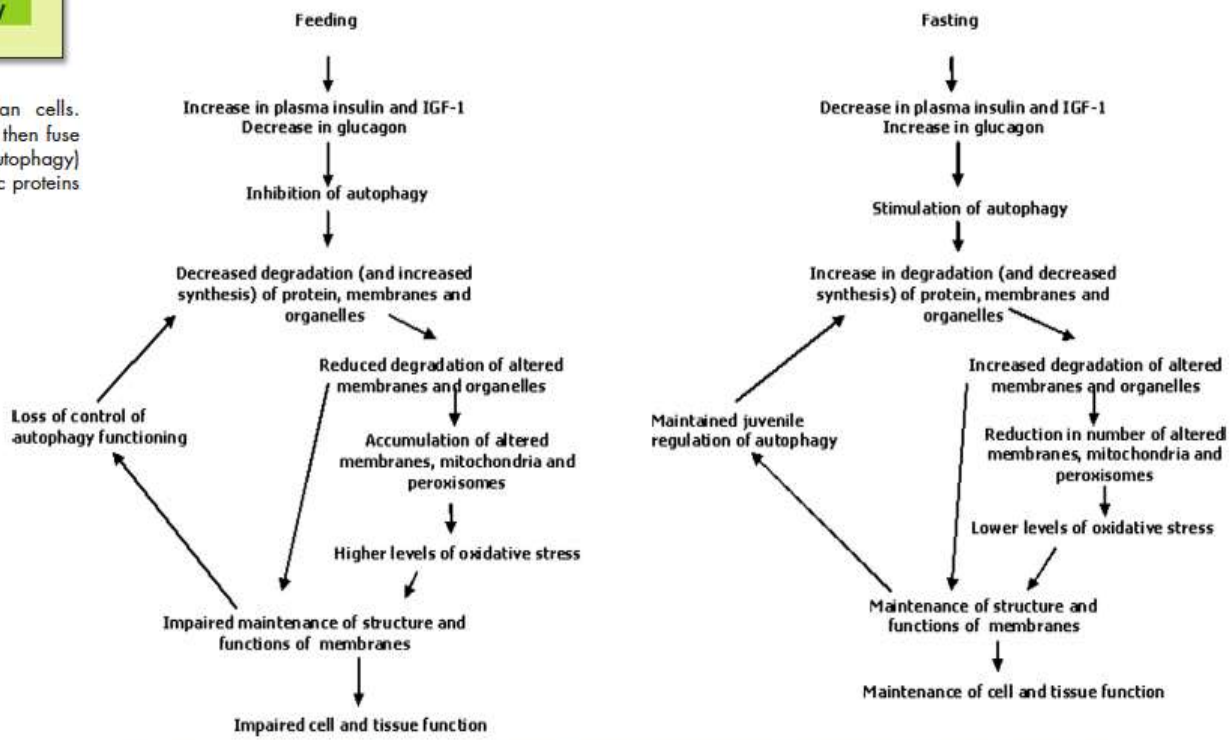

FIGURE 1. Alternation of fast and feeding-time may enhance turnover rate and rejuvenate cells in calorie-restricted rats.

Bergamini E, 2007

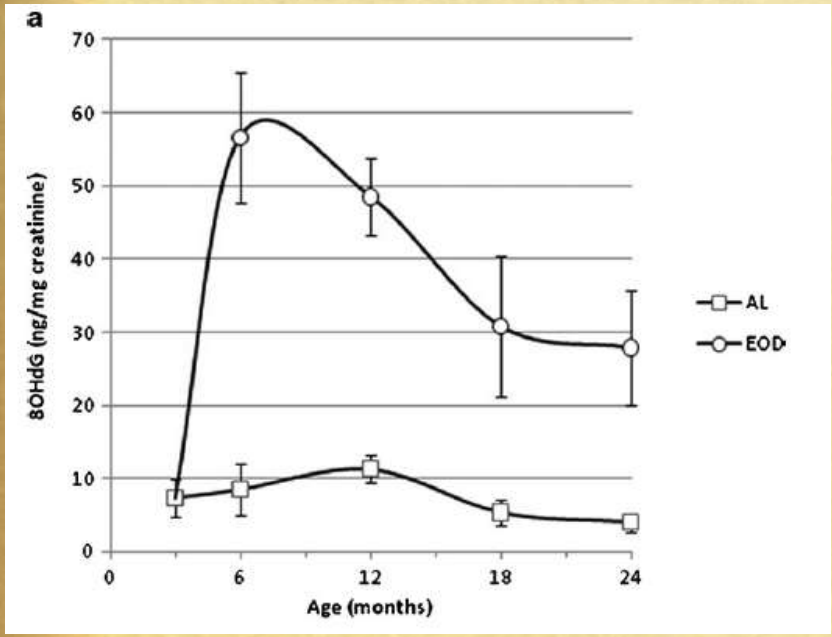

Recupero dell'autofagia da restrizione calorica e

Incremento 8OHdG urinaria come indice di rinnovo mitocondriale

Donati A, 2012

Fig. 3 Effects of the induction of autophagy by DMP administration and of suppression by glucose on urinary 8OHdG. Glucose (1 g/kg body weight) was administered after first DMP injection. Results represent the mean ± SEM of five cases. Two-way ANOVA statistical analysis (nutritional state × DMP): nutritional state main effect, $p<0.0001$; DMP main effect, $p<0.0001$; nutritional state by DMP interaction, $p<0.0001$

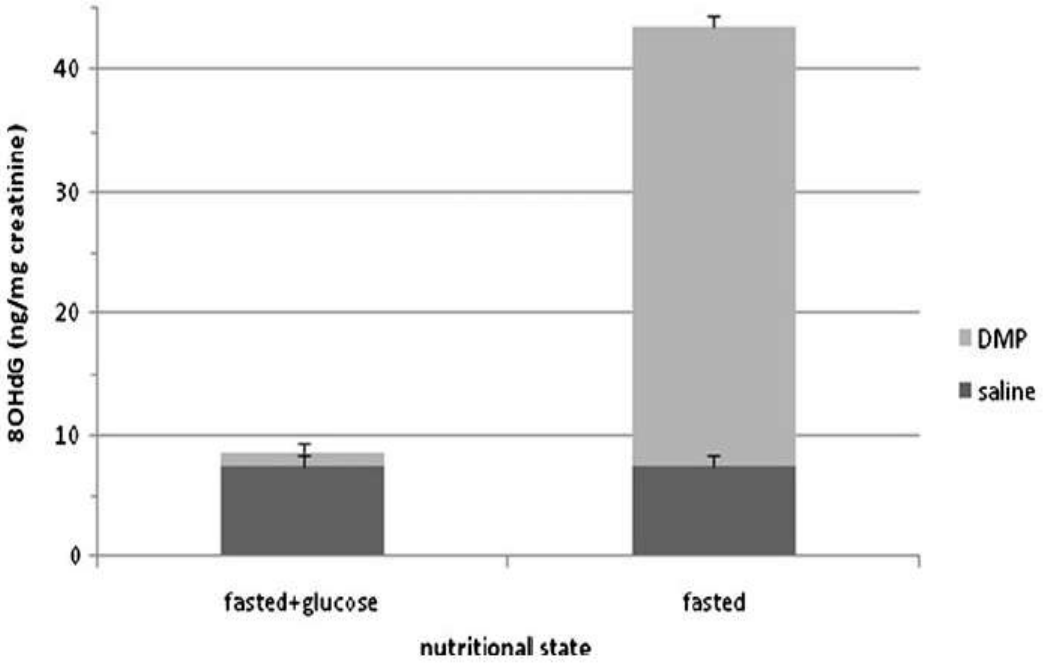

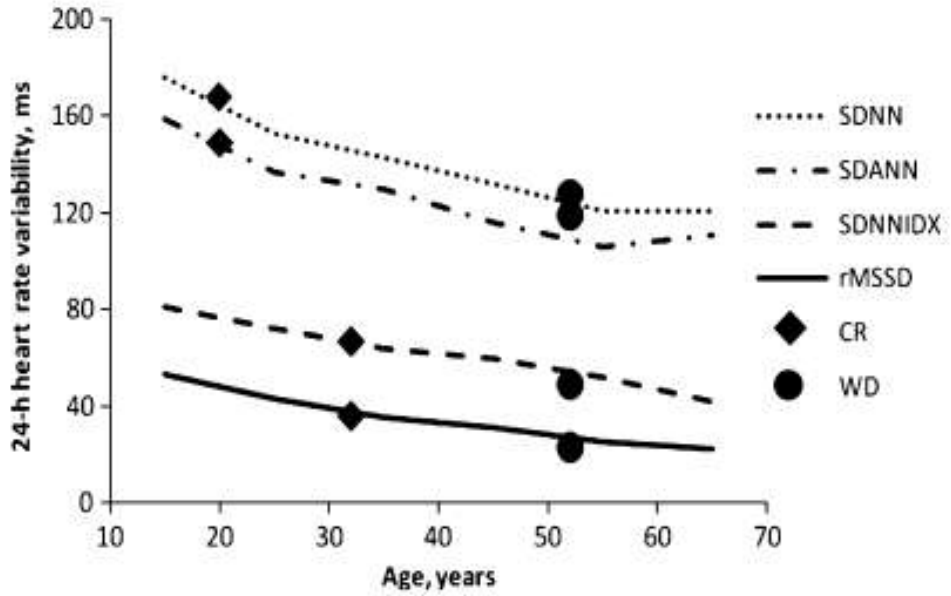

Fig. 1 Mean heart rate variability (HRV) in caloric restriction (CR) (age, 51.5 ± 10.8 years) and Western diets (WD) (age, 52 ± 8.9 years) compared with previously published age-related norms. Curves show age-related norms for 24-h standard deviation of normal-to-normal (N-N) intervals in ms (SDNN), 24-h SD of 5-min-averaged N-N intervals (SDANN), 24-h average of SD of 5-min N-N intervals (SDNNIDX), and root mean square successive difference of N-N intervals in ms (rMSSD) (Umetani *et al.*, 1998). Mean CR HRV values are indicated by filled diamonds and mean WD values by filled circles. See Table 2 legend for HRV definitions.

La restrizione calorica (7 aa.) migliora il profilo del rischio CV (HRV) e la probabilità di morte in soggetti adulti (effetto antiaging in vivo)

Fontana L, 2012
Washington University (S.Louis)

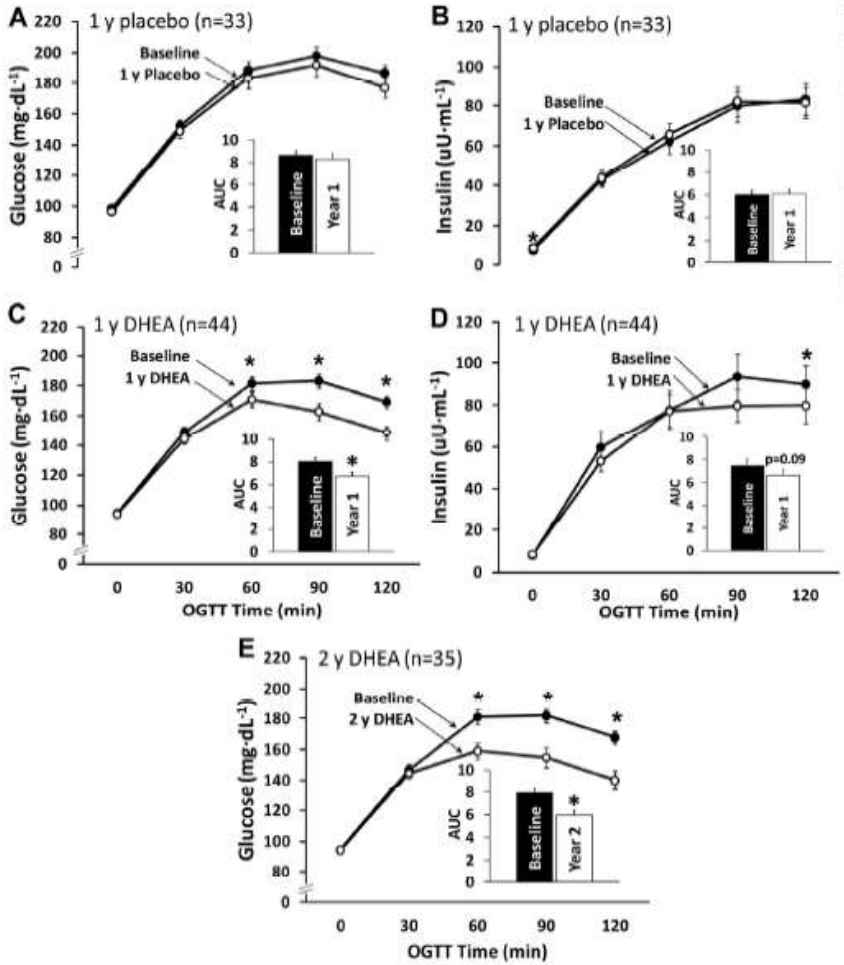

Figure 3. Oral glucose tolerance test results for subjects with abnormal glucose tolerance at baseline. The reduction in the glucose area under the curve (AUC) in the DHEA group (panel C) was significantly greater than that for the placebo group (panel A, p=0.03). Changes in insulin area under the curve did not differ between groups (panels B and D, p=0.52). Improvements in the glucose area under the curve were maintained in a subset of DHEA group participants who underwent a second year of DHEA supplementation (panel E). *p<0.05 for baseline versus DHEA.

Table 3. Circulating Inflammatory Cytokines

	DHEA Group	Placebo Group	Adjusted Difference Between Groups	Between Group *P* value
TNF-α, pg/mL				
Baseline	1.43 ± 0.13	1.34 ± 0.16		
12 months	1.25 ± 0.09	1.62 ± 0.22		
Change	-0.18 ± 0.09	0.27 ± 0.16	-0.43±0.18	0.02
Within group P value	0.18	0.04		
IL-6, pg/mL				
Baseline	2.73 ± 0.20	2.45 ± 0.16		
12 months	2.32 ± 0.15	2.93 ± 0.17		
Change	-0.41 ± 0.13	0.48 ± 0.15	-0.78±0.17	<0.0001
Within group P value	0.004	0.0008		

Abbreviations: TNFα, tumor necrosis factor α; IL-6 interleukine-6

Terapia sostitutiva con DEA per uno-due anni migliora la tolleranza ai carboidrati, la lipidemia, la distribuzione dell'adipe e lo stato subinfiammatorio dei vecchi

Fontana L, 2011

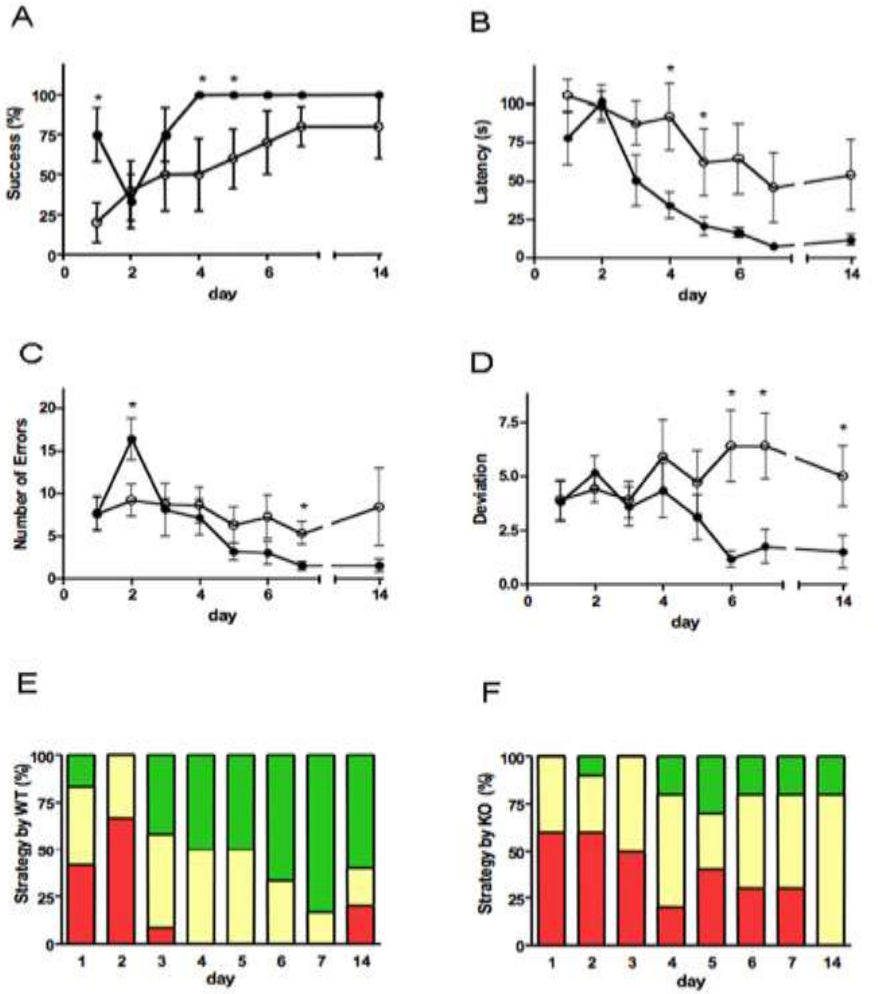

Figure 4.
SIRT1-KO mice show spatial learning and memory impairment.
A, Success of SIRT1-KO mice (n = 5, open) to find the escape box in the Barnes maze was lower than for WT mice (n = 6, * $p < 0.001$, solid). *B*, Latency to find the escape box significantly decreased in WT mice compared to SIRT1-KO (* $p < 0.001$). *C* Number of total errors and *D*, Deviations from the first error (* $p < 0.001$) were both higher in SIRT1-KO mice than WT mice. Search strategy of *E*, WT and *F*, SIRT1-KO mice (serial strategy: yellow, spatial strategy: green and random strategy: red). Data represent means ± SEM. Statistical significance values correspond to the differences between curves analyzed all over the acquisition phase. Asterisks show the days with statistical significance of $p < 0.05$.

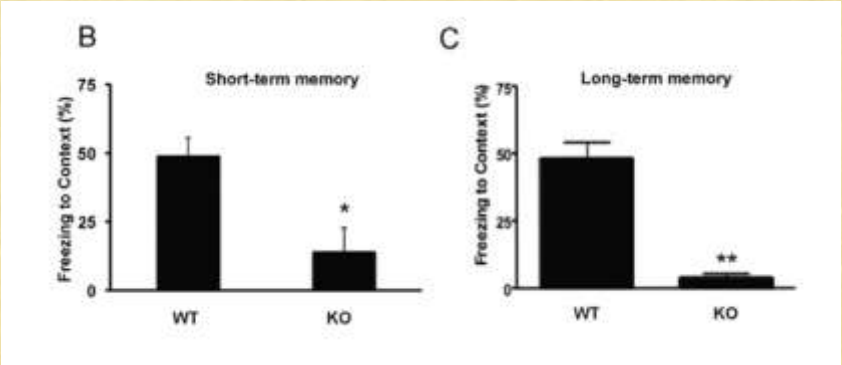

SIRT1 è presente nei neuroni
Nei topi KO per Sirt1 dimostra che la sua attività è indispensabile per il normale apprendimento, la memoria e la plasticità sinaptica

Michan S, 2010
Longo VD

Longo V, 2011

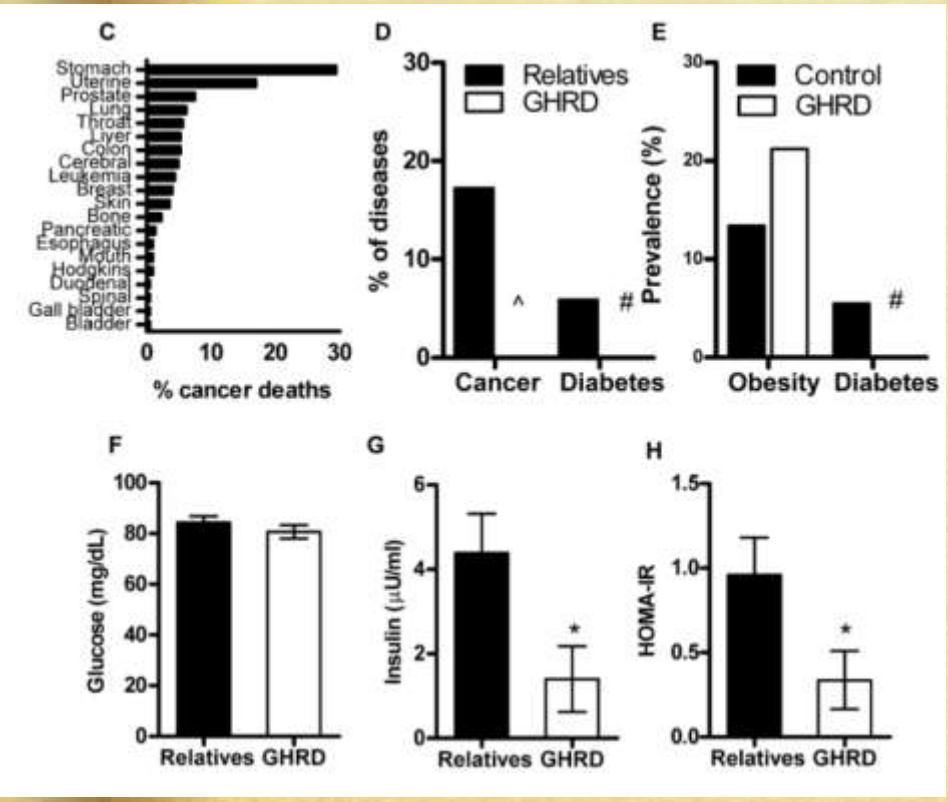

Deficit congenito in GHR e IGF-1 conduce a una minore incidenza di diabete e insulino-resistenza e di cancro

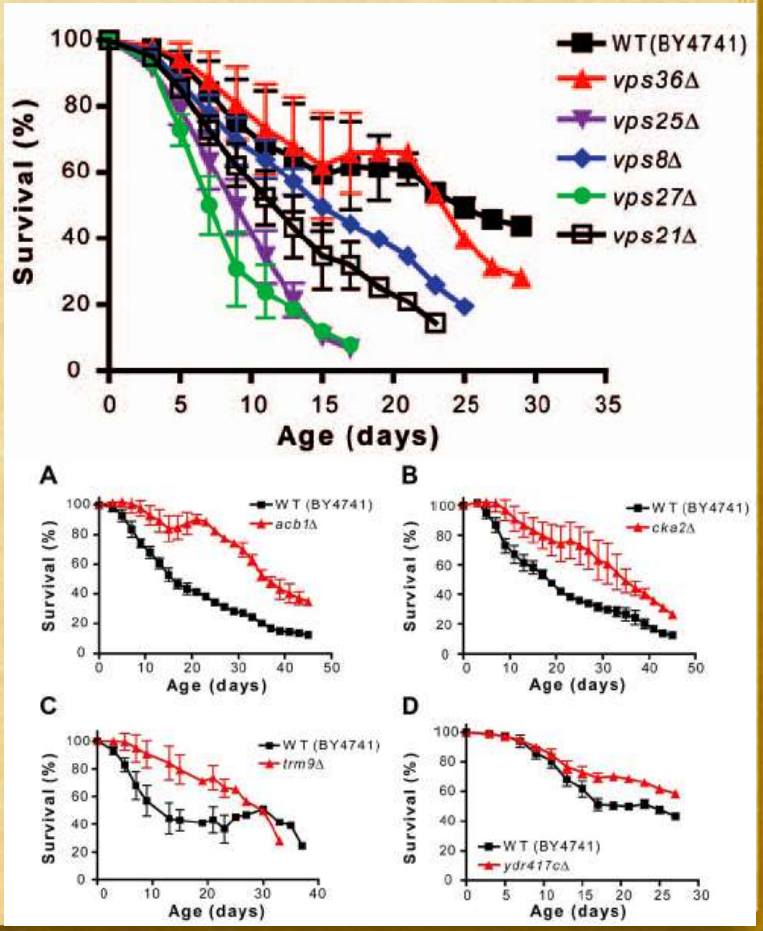

La delezione dei geni che regolano l'autofagia, vacuolar protein sorting, e la respirazione mitocondriale riducono la sopravvivenza; la delezione di geni legati alla sintesi e al trasporto di FFA, al cell signaling, alla metilazione del tRNA allungano la sopravvivenza. Conservati nelle specie: nuovi indicatori dal lievito

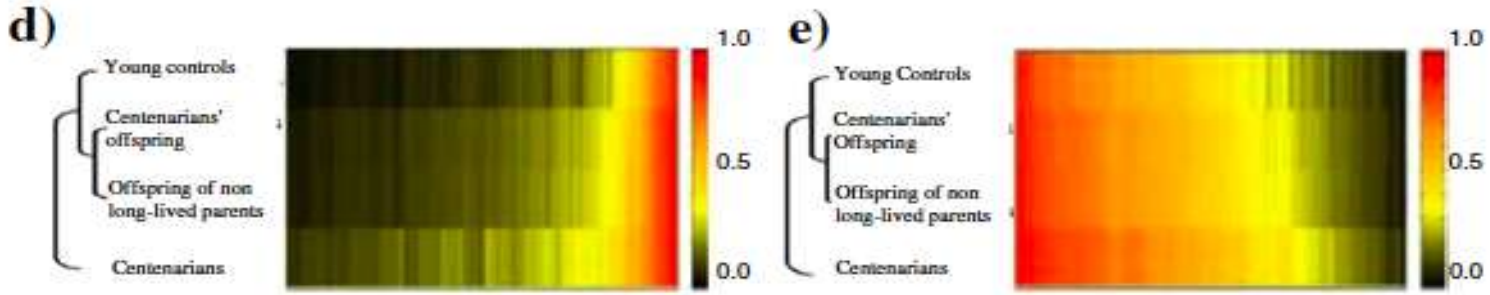

Fig. 2 Aging-associated DNA methylation profile. Venn diagram (**a**) shows the number of CpG loci significantly hyper- and hypo-methylated in centenarians, centenarians' offspring, and offspring of non-long-lived parents vs young controls. Distribution of average (*AVG*) β methylation values of CpG sites over the 709 age-hypermethylated (**b**) and 330 age-hypomethylated (**c**) loci in enrolled populations. Heat map of age-hypermethylated genes (**d**) and age-hypomethylated genes (**e**) in the enrolled populations

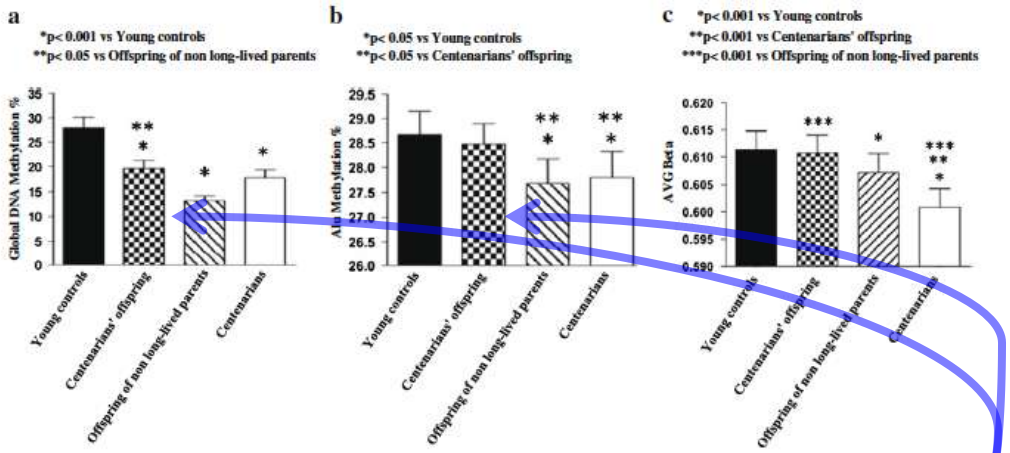

Fig. 1 Global DNA methylation (**a**) and Alu methylation (**b**) in DNA extracted from peripheral leukocytes of young women (n=21), female centenarians' offspring (n=21), female offspring of both non-long-lived parents (n=21), and female centenarians (n=21). Distribution of average (*AVG*) β methylation values of CpG sites localized in non-CpG islands (**c**) in enrolled populations, evaluated by genome-wide array

Ipermetilazione del DNA è presente nei centenari in geni coinvolti nello sviluppo di organi e nella regolazione della trascrizione (cromosomi 5,7,8,13,18)

Ipometilazione del DNA è presente nei centenari in geni coinvolti nella traduzione del segnale, nell'infiammazione e nella difesa dai batteri (cromosomi 1, 20)

Perdita di metilazione del DNA durante l'invecchiamento, ma nei figli di centenari il fenomeno è rallentato

Gentilini D, 2012
(Franceschi C- Mari D)

Table 4
Conditions associated with the presence or absence of digalactosylated or agalactosylated N-glycan structures.

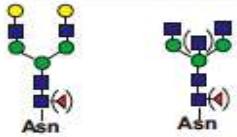

Conditions		
Human conditions		
Age below 60	High	Low
Age above 60	Low	High
Age above 90 (centenarians)	Very low	Very high
Offspring of centenarians	High	Low
Cockaine syndrome	Low	High
Werner syndrome	Low	High
RA and various inflammatory diseases	Low	High
Some epithelial cancers	Low	High
Pregnancy	High	Low
Animal models		
Young mice	High	Low
Old mice	Low	High
Mice under caloric restriction	High	Low
Arthritis in MLR-1lpr/lpr mice	Low	High

For simplicity, it was reported only one digalactosylated N-glycan structure, with or without core-linked fucose (left) and one agalactosylated structure with or without core-linked fucose and bisecting GlcNAc (right). The monosaccharide composition of the two N-linked chains is explained in Fig. 1.

La eccessiva crescita di glicosilazione enzimatica (n-glycome, zucchero legato all'asparagina) è proposto come nuovo marcatore di invecchiamento

Regola infiammazione, risposta immunitaria e vie metaboliche

Dall'Oglio F, 2012
(Franceschi C)

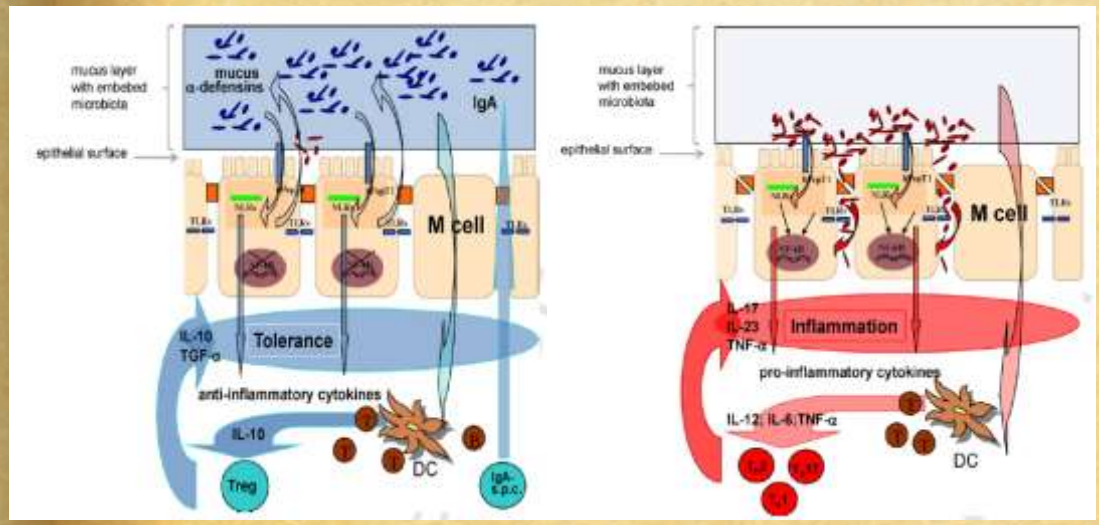

Gli enterociti hanno sistemi di riconoscimento dei batteri e rispondono strategicamente sulla base della carica con citochine, risposte immunitarie, IGA secretorie, ecc
Invecchiamento compromette una risposta "propozionata" e si sposta verso un'infiammazione cronica

Biagi E, 2012
Franceschi C

miR21 è maggiormente espresso e in più alta concentrazione nel gruppo >70 anni, regola l'espressione del recettore per TGFbeta

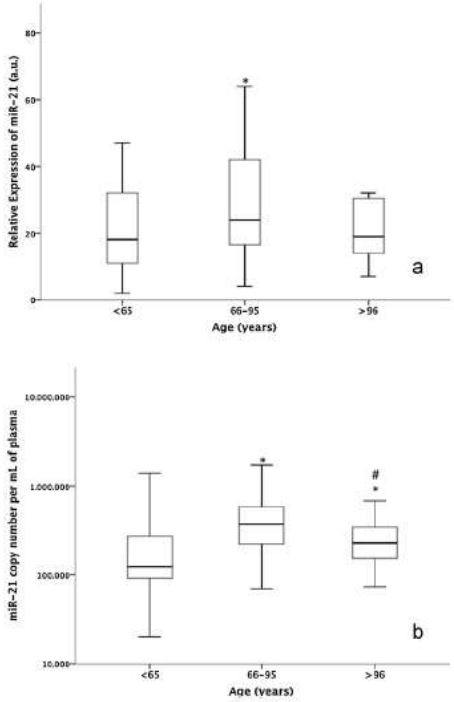

Fig. 5. Circulating miR-21 expression in the CTR subjects (stratified by age group). (a) The relative expression of circulating miR-21. $^{*}p < 0.05$ vs. <65 years. The relative expression of miR-21 was calculated using the following equation: $2^{-\Delta Ct}$, in which ΔCt = Ct miR-21 − Ct miR-17-5p. (b) The absolute expression of circulating miR-21. $^{*}p < 0.05$ vs. <65 years, $^{\#}p < 0.05$ vs. <66–95 years. The absolute concentration of miR-21 (expressed as the "number of molecules per ml of plasma") was determined by diluting known input quantities of synthetic miR-21.

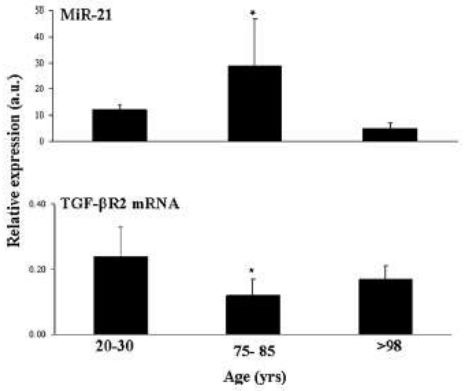

Fig. 9. The expression of miR-21 and TGF-βR2 mRNA in the leukocytes of young subjects, old subjects and centenarians. The levels of miR-21 and TGF-βR2 mRNA in the leukocytes of 5 individuals aged 20–30 years, 5 individuals aged 75–85 years and 5 centenarians. The data were normalized against β-actin levels and are reported as the mean value ± S.D.

Olivieri F, 2012
Franceschi C

miR21 è più alto nei soggetti affetti da patologie CV e più basso nei centenari

Marcatore di invecchiamento e di infiammazione

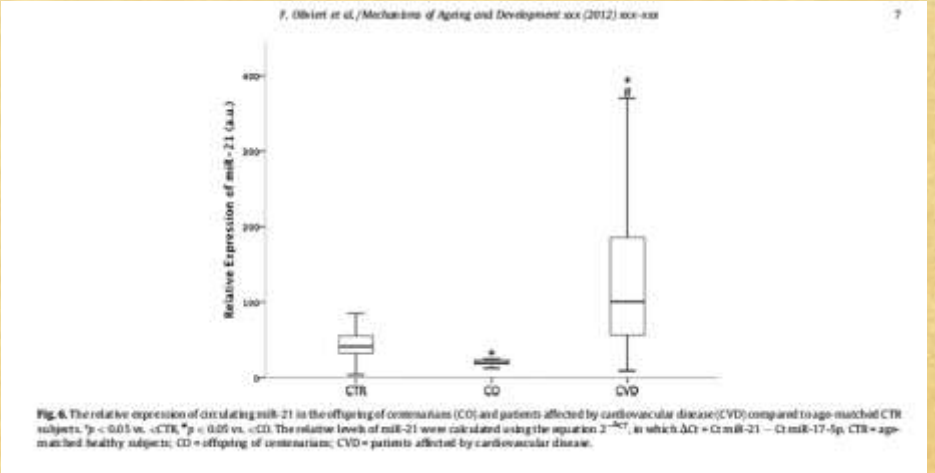

Fig. 6. The relative expression of circulating miR-21 in the offspring of centenarians (CO) and patients affected by cardiovascular disease (CVD) compared to age-matched CTR subjects. $^{*}p < 0.05$ vs. <CTR, $^{\#}p < 0.05$ vs. <CO. The relative levels of miR-21 were calculated using the equation $2^{-\Delta Ct}$, in which ΔCt = Ct miR-21 − Ct miR-17-5p. CTR = age-matched healthy subjects; CO = offspring of centenarians; CVD = patients affected by cardiovascular disease.

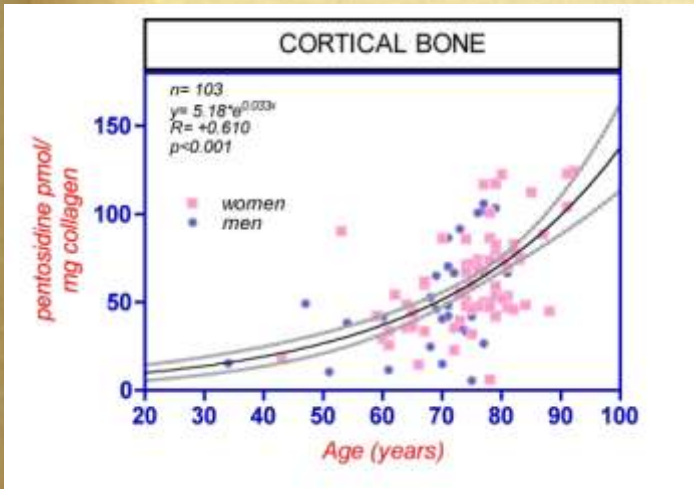

Monacelli F, 2012 , Sanguineti R
Odetti P

Ruolo nella evoluzione della placca ATS

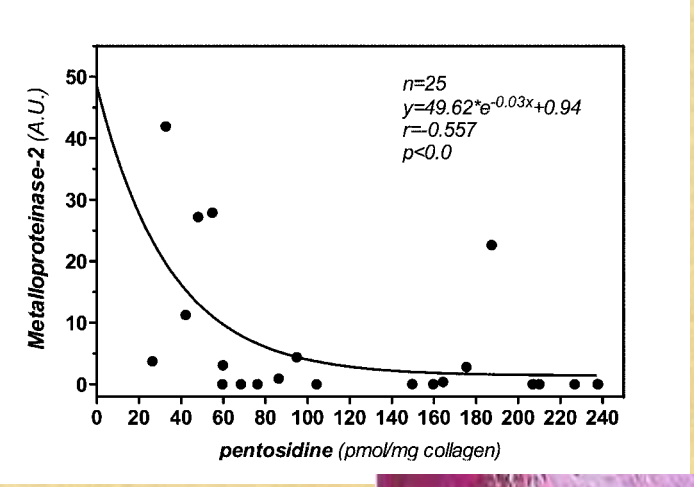

Accumulo di AGEs con l'invecchiamento responsabile di osteoporosi e di inibizione della formazione di osso

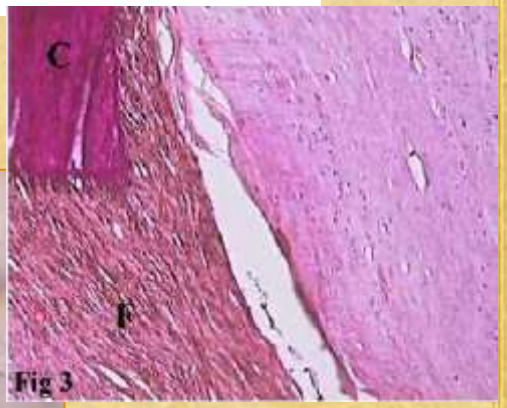

contro llo

0,25 nmol/ml pentosidina

1 nmol/ml pentosidina

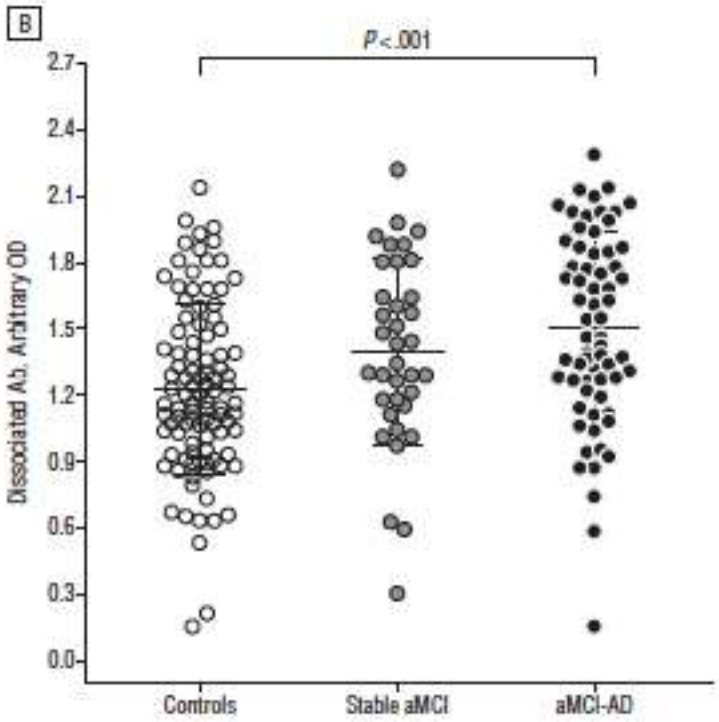

Anticorpi circolanti anti Abeta più alti nei soggetti con MCI- che evolveranno verso AD

Storace D, 2010

Odetti P

Table 5
The top 10 variables with their input relevance

Variable	Input relevance
Glycemia	23.4
HOMA2	22.4
Female	18.8
ApoE $\varepsilon 3/\varepsilon 4$	18.7
Attentional matrices	16.7
Short story	15.7
Insulin	15.0
$A\beta_{42}$	12.9
Praxis	11.7
ApoE $\varepsilon 4/\varepsilon 4$	11.6

In un sistema di valutazione del rischio di AD, analizzato con ANN, i fattori metabolici sono i principali predittori di AD

Odetti P

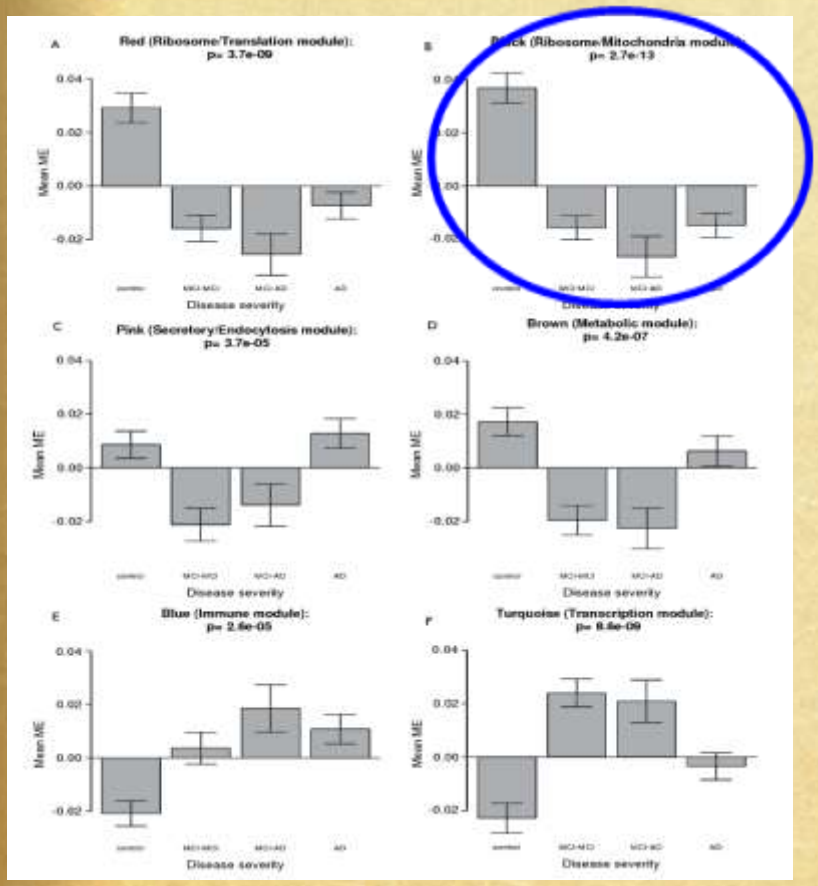

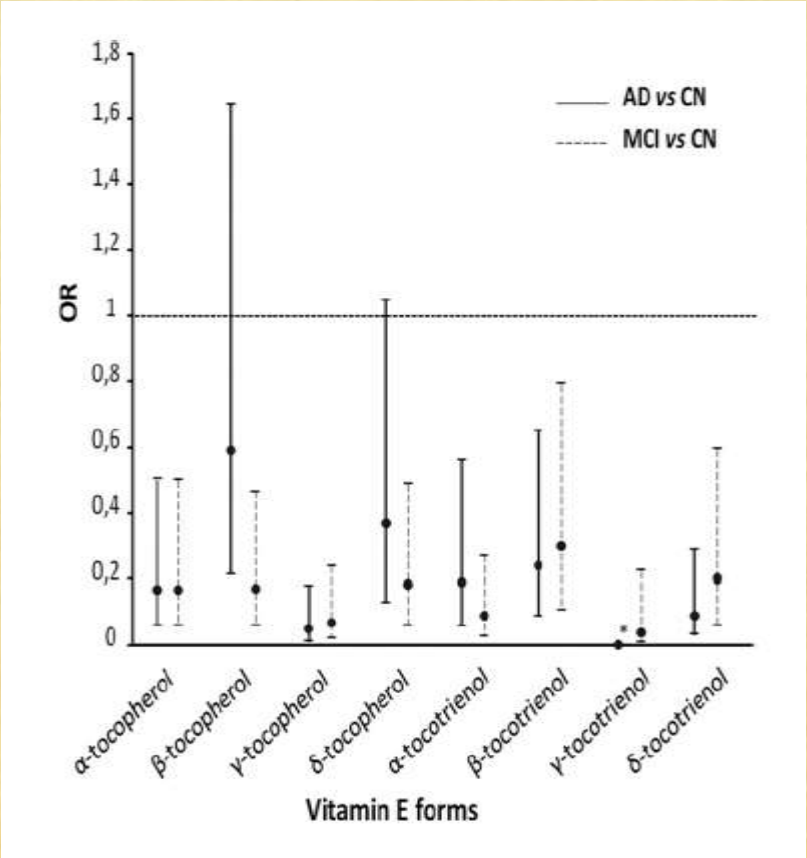

Lunnon K, 2012

Mecocci P

Mangialasche F, 2012

Espressione genica in cellule del sangue in MCI e AD dimostra che esiste una reazione cellulare periferica alla patologia
Forte evidenza che esista una disfunzione mitocondriale (riduzione espressione complessi respiratori)
Altre: immunologiche, metaboliche, trascrizionali, …

Bassi livelli di tocoferoli e tocotrienoli sono presenti sia nei soggetti con MCI che in quelli con AD
Avrebbero effetto protettivo sul SNC e averli bassi ha significato predittivo per decadimento cognitivo

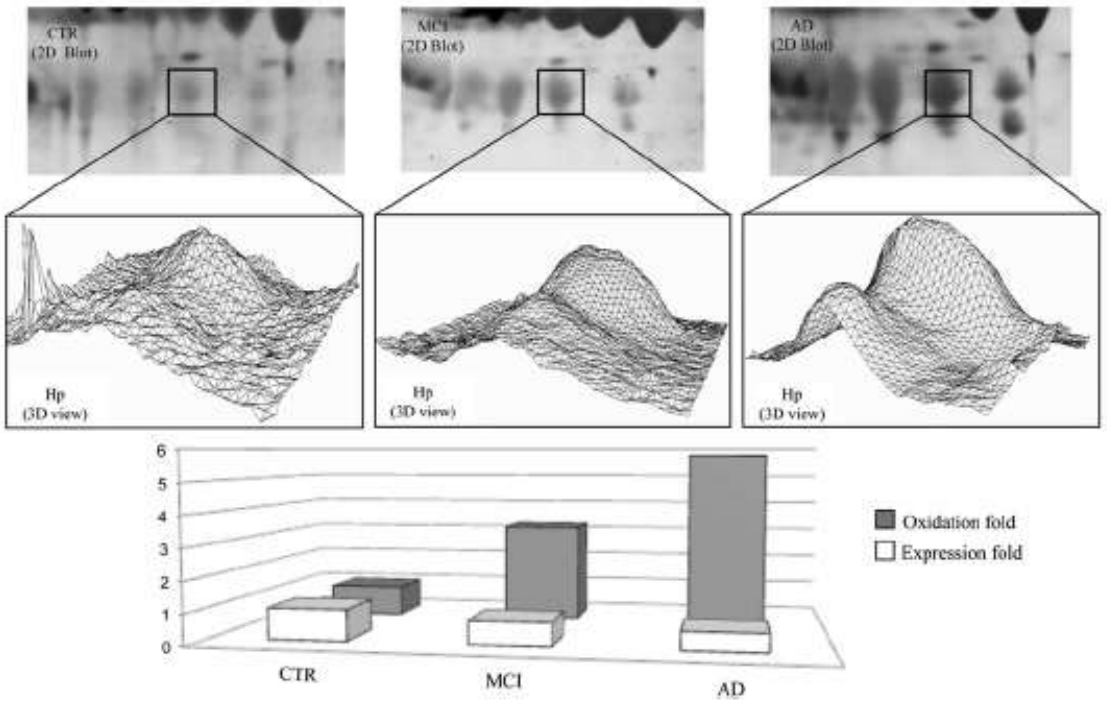

Fig. 4. Hp β-chain oxidation fold. At the top an enlarged area of 2D blot from each group, CTR, MCI, and AD, is shown corresponding to the Hp train of spots. The Hp β-chain spot identified as differentially oxidized in the three groups is labeled. 3D density graphs were elaborated by PDQuest from the Hp spot on the 2D blot. At the bottom the histogram reports both expression levels and oxidation fold for Hp β chain (data obtained from proteomics and redox proteomics approaches).

Cocciolo A, 2012
Mecocci P

L'aptoglobina in corso di MCI o AD perde la sua funzione di proteina chaperon per riduzione della sintesi o perché ossidata
Non riesce a inibire la formazione di fibrille Abeta

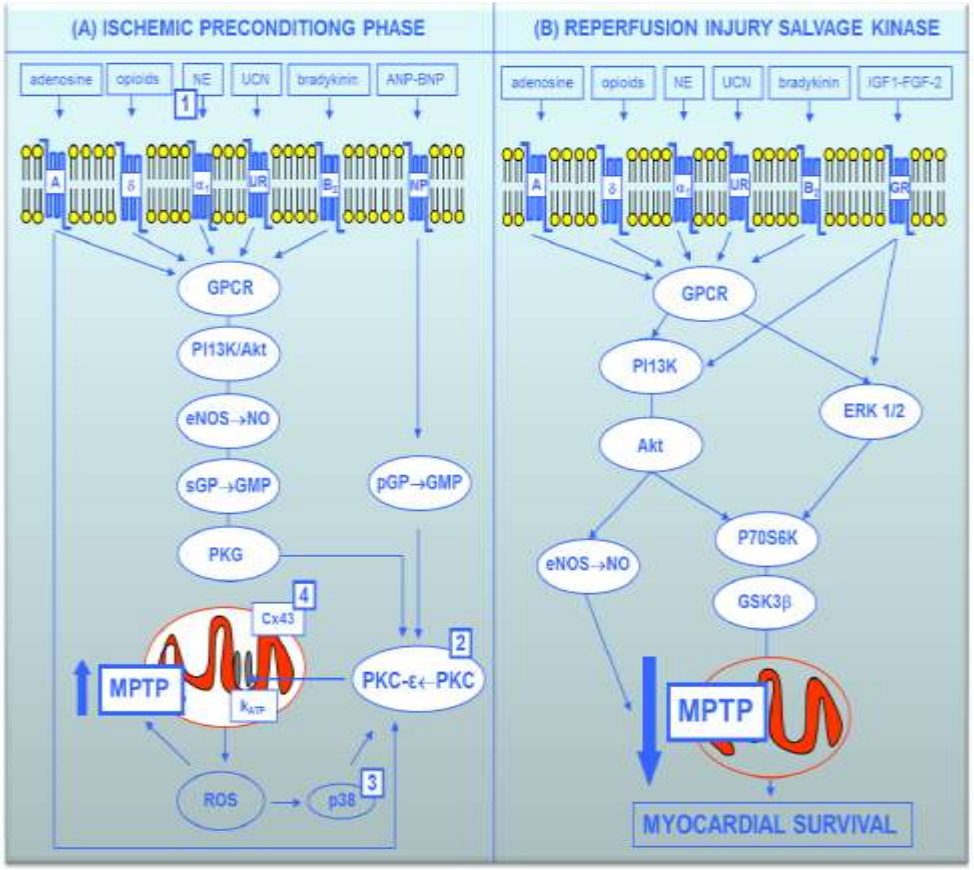

Fig. 1: Hypothetical mechanism of IP-induced cardioprotection (see text for details). (A) Ischemic preconditioning phase: NE=Norepinephrine; UCN=Urocortins; ANP=Atrial Natriuretic Peptide; BNP=Brain Natriuretic Peptide; GPCR=G-protein coupled receptor; NPR, natriuretic peptide receptor; PI3K=Phosphatydil-inositol 3 kinase; Akt=serine/threonine kinase; serine/threonine kinase eNOS=endothelial Nitric Oxide Synthase; NO=Nitric Oxide; sGC=soluble Guanylate Cyclase; GMP=Guanosine MonoPhosphate; pGC=particulate Guanylate Cyclase; PKG=Protein Kinase G; PKC=Protein Kinase C; Cx43=Connexin 43; K_{ATP}=Mitochondrial potassium ATP-dependent channels; ROS=Reactive Oxygen Species; MPTP=Mitochondrial Permeability Transition Pore; p38=p38 mitogen-activated protein kinase. (B) Reperfusion Injury Salvage Kinase (RISK): IGF-1, insulin-like growth factor; FGF-2, fibroblast growth factor 2; GFR=Growth Factor Receptor; ERK=extracellular regulated kinase; P70S6K=p70 ribosomal S6 protein kinase; GSK3ß=glycogen synthase kinase 3beta. In (A), the numbers in squares indicate the age-related IP impairment sites: 1=Abete et al., 1996; 2=Tani et al., 2001; 3=Fenton et al., 2005; 4=Boengler et al., 2007 (with permission, Abete P et al., 2010) [56].

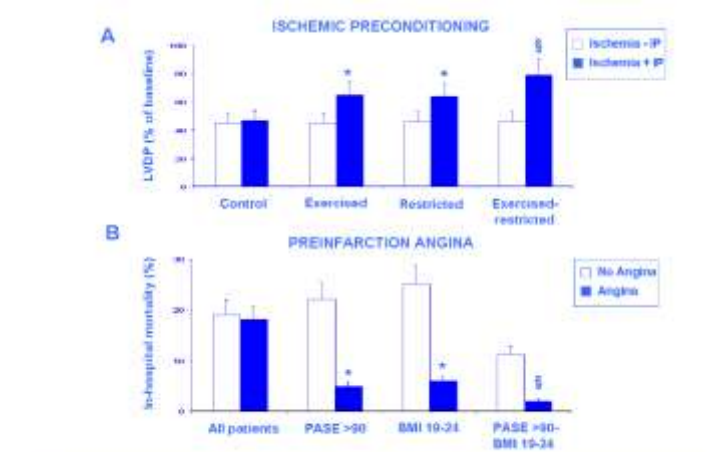

Fig. 4: The restoration of the age-related of IP by exercise training and caloric restriction in the isolated and perfused rat heart is shown in panel A. Bar graphs show the recovery of left ventricular developed pressure (LVDP) (% of basal) at the end of reperfusion in sedentary ad libitum fed (control), trained ad libitum fed, sedentary food-restricted and trained- and food-restricted senescent hearts subjected to ischemia (20 min) and reperfusion (40 min) (Ischemia - IP) and pre-treated with preconditioning stimulus of 2 min followed by 10 min of reperfusion (Ischemia + IP). LVDP recovery was similar in the absence and the presence of IP. Exercise training and caloric restriction restored IP ($p<0.01$ vs. Control) and this effect was more evident in hearts from trained- and food-restricted rats ($^{\S}p<0.001$ vs. Control). The preservation of the age-related reduction of the cardio-protective effect of preinfarction angina, a clinical equivalent of IP, by physical activity evaluated by Physical Activity Scale for the Elderly (PASE) score and by a normal body-mass index (BMI) is shown in B. Bar graphs show that in-hospital mortality percentage was similar in elderly patients without and with preinfarction angina but it was lower in elderly patient with preinfarction angina with high PASE score (>90) and normal BMI (19-24) ($^{\S}p<0.05$ vs. all patients). This effect was more evident in elderly patients with the highest PASE (>90) and the normal BMI (19-24) (*$p<0.01$ vs. all patients) (with permission, Abete P et al., 2010) [56].

Precondizionamento ischemico si riduce con l'età, ma il complesso meccanismo si può riattivare con la restrizione calorica e con l'esercizio fisico (e ancora con più efficienza con entrambi)

Abete P, 2011
Rengo F

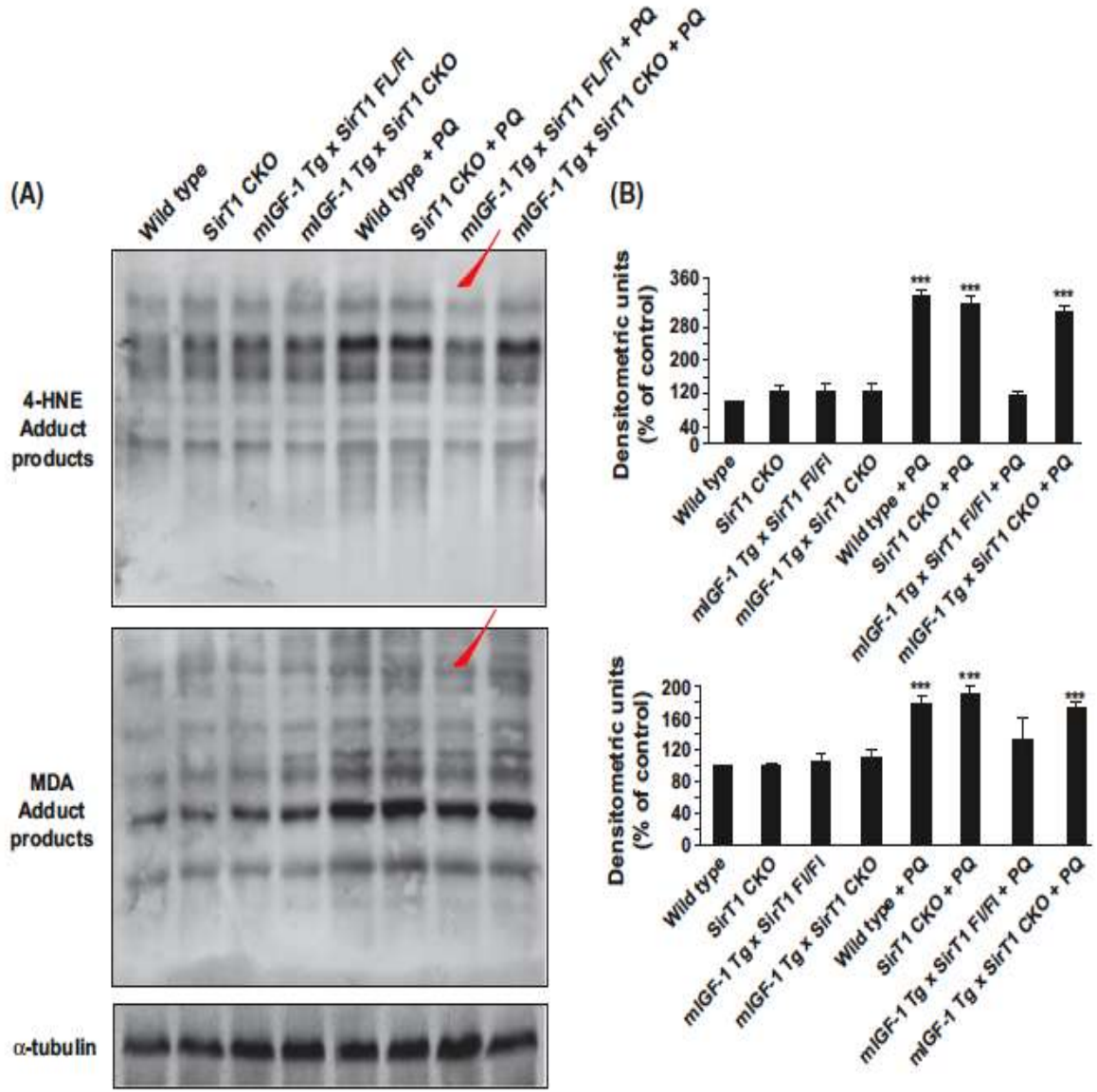

Il propeptide IGF1 è implicata nella protezione cardiaca inducendo l'espressione di Sirt1 (deacetilasi)
Inibendo lo stress ossidativo legato allo scompenso cardiaco in età avanzata

Vinciguerra M, 2012
Rosenthal N

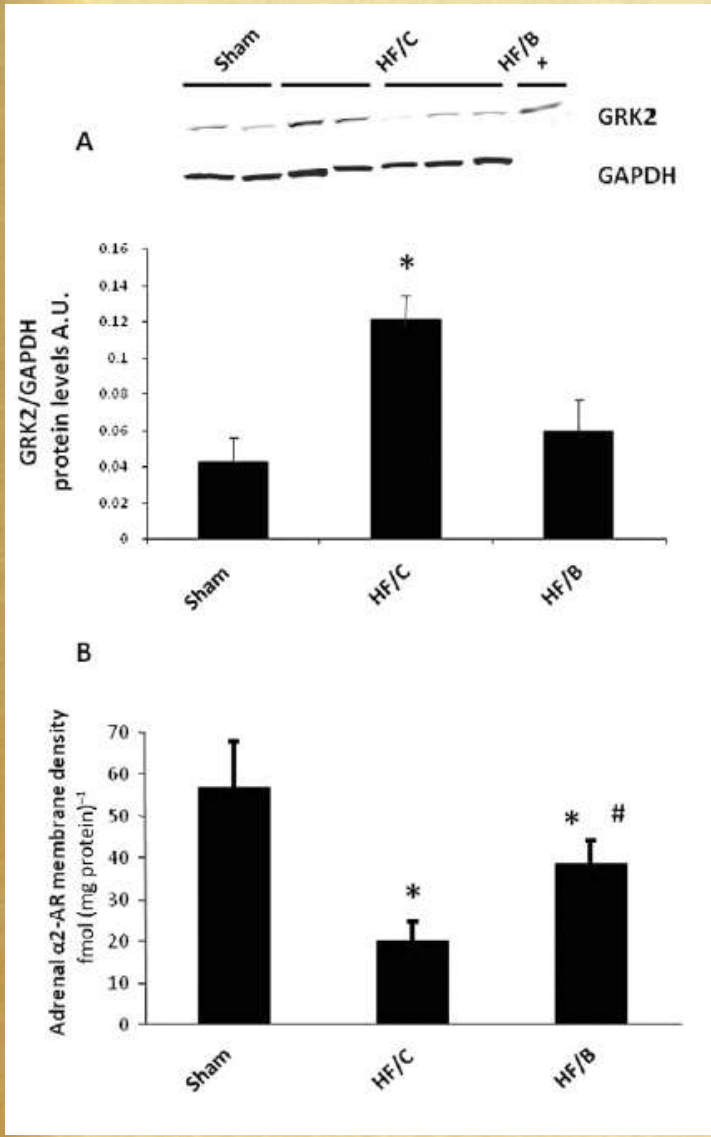

L'iperattività del sistema adrenergico peggiora il quadro fisiopatologico dello scompenso cardiaco che i beta bloccanti migliorano

Viene dimostrato in ratti (a cui è stato provocato un infarto miocardico) che il meccanismo dei beta bloccanti per ridurre l'iperattività simpatica è mediato dalla riduzione dell'attività della GPCR kinase-2 surrenalica, iperespressa in corso di scompenso cardiaco. La consequenza è anche una riduzione di catecolamine circolanti

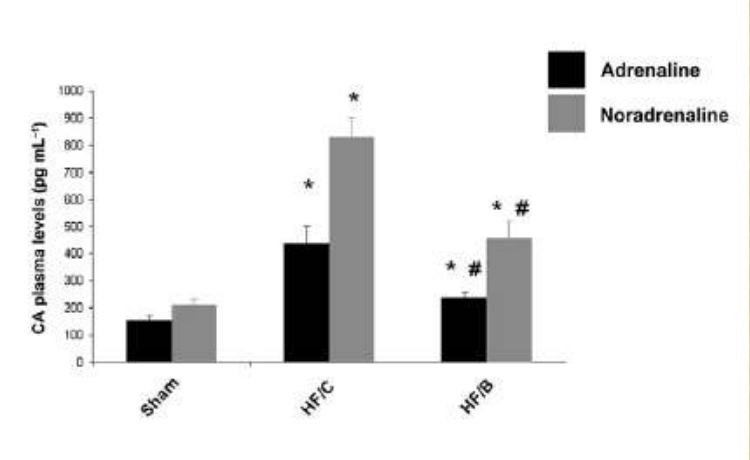

Leosco D., 2012

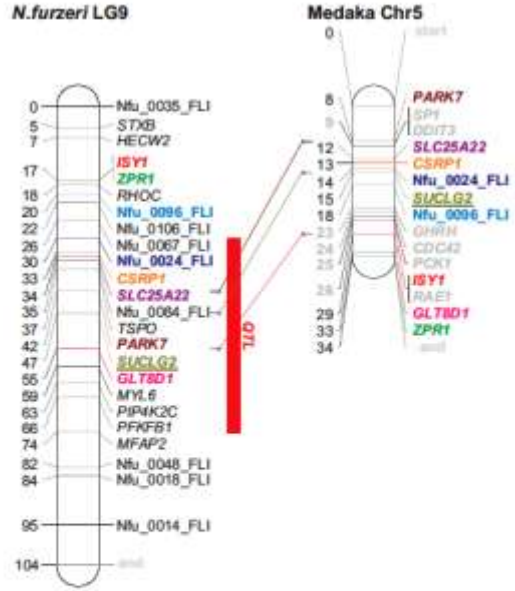

Fig. 5 Cross-species analysis of *Nothobranchius furzeri* LG 9 (in cM) and medaka Chr 5 (in Mb). The red bar on the right of LG 9 represents the 95% confidence interval of the highly significant lifespan QTL. Nine markers (colored) of *N. furzeri* LG 9 were assigned to medaka Chr 5, including the peak marker (*SUCLG2*) and flanking genes (*PARK7* and *GLT8D1*). Three colored lines indicate their respective location on the *Nothobranchius furzeri* LG 9 and medaka Chr 5. Six human orthologs of aging-relevant genes (gray) were assigned to this medaka region. Gene names and gene-associated markers are given in italics. Microsatellite markers are given in the following way: Nfu_number_FLI. QTL, quantitative trait locus; LG, linkage group.

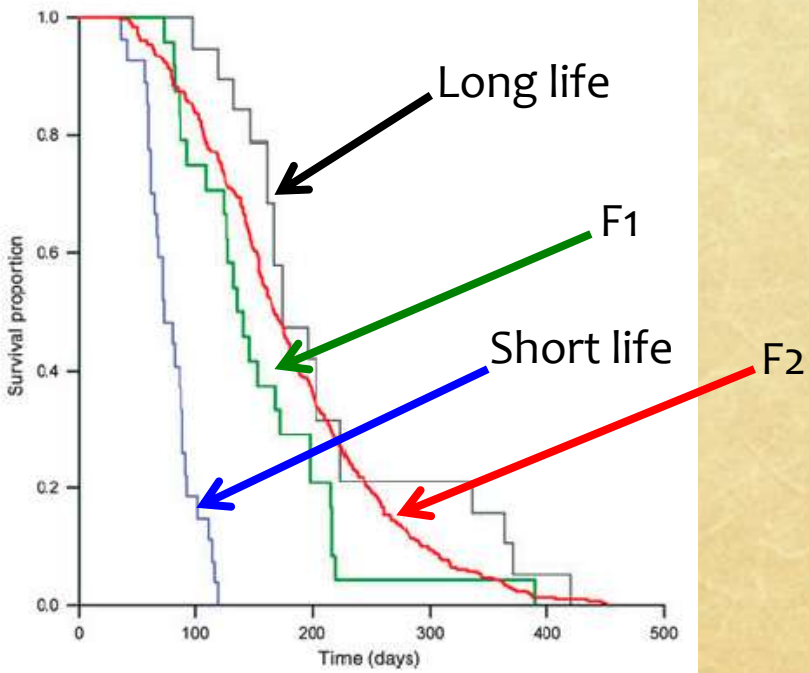

Fig. 2 Survivorship of cross AB and GRZ (n = 27, blue) and MZM-0403 (n = 19, black), as estimated by Kaplan–Meyer analysis. F_1 progeny (n = 24) is given in green; F_2 (n = 310) progeny is shown in red. The mean and maximum lifespans of GRZ and MZM-0403 were significantly different ($P < 0.001$, log-rank test). The F_1 progeny showed an intermediate and significantly different lifespan compared with both parental strains ($P < 0.001$). The F_2 offspring had a longer mean and maximum lifespan than GRZ and F_1 progeny, but less compared with MZM-0403, and was significantly different only from GRZ ($P < 0.001$).

Nel pesce N. furzeri i loci genetici che controllano la longevità sono stati identificati incrociando ceppi con breve e lunga vita (3 anni) dando supporto alla linea di ricerca su modelli genetici di controllo della longevità

Kirschner J,2012
Cellerino A

Table 2. Effect of zinc supplementation in the elderly in accordance with genetic background and zinc status

	Parameter	Effect of the zinc supplementation	General causes of variability observed
Zinc status[48,70]	Plasma zinc	↑	Plasma zinc levels before supplementation, inflammatory status, country (dietary habits), IL-6 −174 and MT1A +647 polymorphisms
	Plasma zinc/albumin	↑	Plasma zinc levels before supplementation, inflammatory status, country (dietary habits), IL-6 −174 and MT1A +647 polymorphism
	Labile intracellular zinc	↑↑	IL-6 −174 polymorphism, country (dietary habits)
	MT	↑	IL-6 −174 and MT1A +647 polymorphisms, country (dietary habits),
	Nitric oxide-induced release of zinc	↑↑	IL-6 −174 polymorphism, country of origin (dietary habits)
	Granulocyte zinc	↑↑	IL-6 −174 polymorphism, country (dietary habits)
	MT glutathionylation	–	–
Stress-related proteins[48,88]	Poly(ADP-ribosyl)ation capacity	↑	Plasma zinc levels before supplementation and increase of plasma zinc after supplementation
	Reactive oxygen species production	↓	Plasma zinc levels before supplementation, age of donors
	ApoJ plasma	–↑	IL-6 −174 polymorphism, country (dietary habits)
	Genes involved in nitrosative stress (ATF2, CSF2, FOS, ICAM1, JUN, LTA, CCL2, SELE, VCAM1, inducible nitric oxide synthase, TNF and NFκB1)	↓	–
	Total intracellular carbonyl levels	↓	–
	MsR activity and protein expression	↑↑	Country (dietary habits)
	Chymotrypsin-like peptidase activity of proteasome and 20S protein expression	↑	–
	Chaperone (heat-shock protein 72) protein levels	–↑	–
	Chaperone (heat-shock protein 72) inducibility	↑↑	–
			–
Antioxidant plasma enzymes[48]	Plasma SOD	↑	–
	Erythrocyte SOD	↑	–
	Catalase	↓	–
	Glutathione peroxidase	↓	–
Thymic output[48]	T-cell receptor excision circles	↓↑	Age, gender, country (dietary habits), plasma zinc at baseline
Senescence and apoptosis[48]	Telomere length	–↑	Country (dietary habits)
	Early spontaneous apoptosis	↓	P53 codon 72 polymorphism
	Late apoptosis	↓	
	Oxidative stress-induced apoptosis	↓	
	Mitochondrial membrane depolarization during spontaneous and dRib-induced apoptosis	↓	
	Cell cycle	–	
Plasma cytokines/ chemokines[89]	IL-6, IL-8 and MIP-1α	–↑	Gender, country (dietary habits), plasma zinc at baseline, IL-6 −174 and MT1A +647 polymorphism
	MCP-1 and RANTES	–	Gender, country (dietary habits), plasma zinc at baseline, IL-6 −174 and MT1A +647 polymorphism
Immune functions[89]	NK lytic activity	↑↑	–
	Basal IFN-γ, IL-8, IL- 1ra and IL-6 production	↓	–
	Basal IL-10 and TNF-α production	↓	–
	Stimulated IFN-γ, IL-6, TNF-α, IL-1ra and IL-10 production	↑	–
Jak/Stat signalling and immunomodulation[48,89]	IL-2 and IL-6 STAT3 and STAT5 activation	–	Age of donors, basal zinc status
	Activation-induced cell death	↑	Age of donors, basal zinc status
	Cytokines and metabolic gene expression response to zinc	↑↓	Age, gender and IL-6 −174 and MT1A +647 polymorphism
T cells subsets[89]	Activated T cells (CD3+CD25+)	↓	–
	CD4:CD8	–	–
	Frequencies of CMV-specific cells	–	–

MT, metallothionein; ATF2, activating transcription factor 2; CSF2, colony stimulating factor 2; ICAM1, inter-cellular adhesion molecule 1; LTA, lymphotoxin-α; CCL2, chemokine (C-C motif) ligand 2; SELE, E-selectin; VCAM1, vascular cell adhesion molecule 1; MsR, methionine sulfoxide reductase; SOD, superoxide dismutase; dRib, 2-deoxy-D-ribose; MIP-1α, macrophage inflammatory protein 1α; MCP-1, monocyte chemotactic protein-1; RANTES, regulated upon activation normal T-cell expressed and secreted; CMV, cytomegalovirus; ↑↑ = strongly increased, ↑ = increased, – = not modified, –↑ = slightly increased at least in some sub-groups, ↑↓ = great inter-individual variability.

Animali con metallotionine iperespresse (antiossidanti) non vivono molto più a lungo se non in un ambiente arricchito di zinco,

Mocchegiani E, 2010

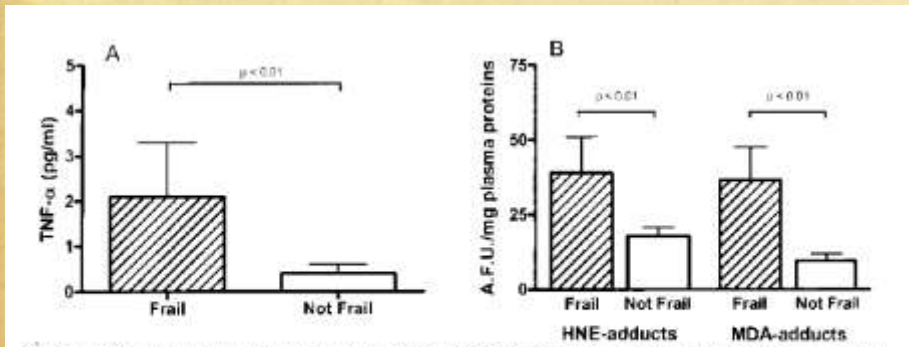

Fig. 2. A) TNF-α concentrations in plasma of Frail and not frail; B) plasma level of aldehyde-protein adducts in Frail and non frail people. MDA and HNE fluorescent adducts were recorded using 390/460 and 355/460 nm of emission/excitation wavelength respectively. Data are expressed as means ± SDM. P values refer to the results of the unpaired Student's T test. (A.F.U.: Arbitrary Fluorescence Units.

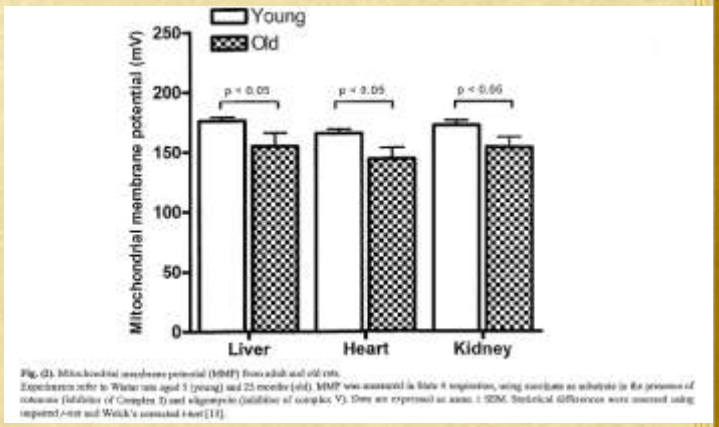

Fig. (3). Mitochondrial membrane potential (MMP) from adult and old rats.
Experiments refer to Wistar rats aged 3 (young) and 23 months (old). MMP was measured in fresh 4 mg/mitochondria, using succinate as substrate in the presence of rotenone (inhibitor of Complex I) and oligomycin (inhibitor of complex V). Data are expressed as means ± SDM. Statistical differences were assessed using unpaired t-test and Welch's corrected t-test [14].

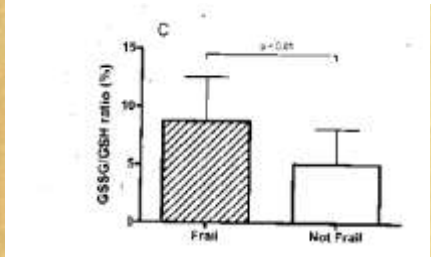

Fig. 1. Changes in oxidized (A) / reduced (B) blood Glutathione levels and GSSG/GSH ratio (C) in FS and non-frail people. Data are expressed as means ± SDM. P values refer to the results of the unpaired Student's T test.

b. Nei soggetti anziani fragili è aumentato lo stress ossidativo come evidenziato dagli addotti MDA e HNE, dal rapporto GSSG/GSH e dall'aumento di TNF-alfa

a. Nell'animale esiste con l'invecchiamento un danno del mitocondri con aumento dello stress ossidativo

Vendemiale G, 2007-9

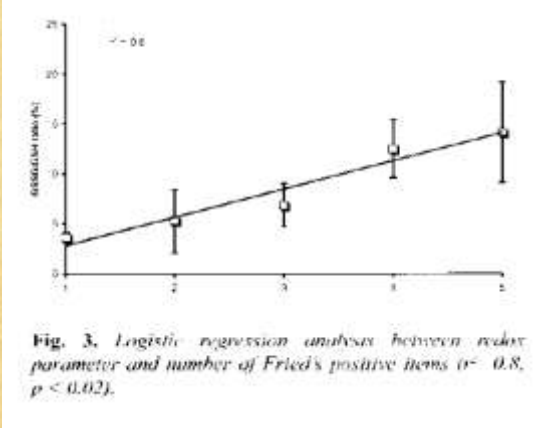

Fig. 3. Logistic regression analysis between redox parameter and number of Fried's positive items (r= 0.8, p < 0.02).

c. La regressione lineare tra i punti della scala Fried e il rapporto GSSG/GSH porta ulteriore sostegno alla relazione

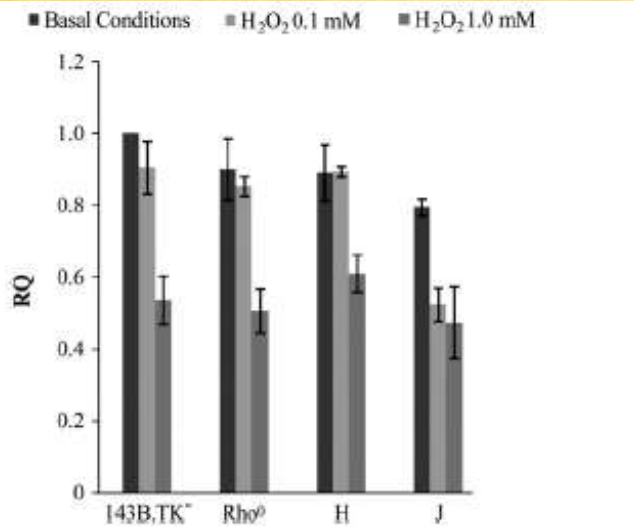

Fig. 1. mRNA levels of the *SIRT3* gene measured in 143B.TK⁻, Rho⁰ and cybrid cell lines at both basal and stress conditions. These levels are reported as the mean of Relative Quantification values (RQ), measured in three independent triplicate experiments with standard error mean (SEM).

Cellule cybrid J più protette da stress ossidativo

D'aquila P., 2012

Passarino G.

Rose G, 2011

Table 4. Estimation of haplotype frequencies in the *UCPs* SNPs and association with longevity in the analyzed sample.

Gene	SNPs			Freq[a]	Score	P-value[b]
UCP2-UCP3	**rs660339**	**rs659366**	**rs15763**			
	C	A	C	0.029	−2.876	0.003
	C	G	C	0.596	−1.747	0.086
	C	G	T	0.028	0.317	0.754
	C	A	T	0.004	0.877	0.400
	T	A	C	0.077	0.953	0.347
	T	G	C	0.050	0.971	0.339
	T	A	T	0.184	1.390	0.165
	T	G	T	0.030	1.985	0.046
UCP3	**rs15763**	**rs1800849**				
	C	C		0.659	−3.720	<0.001
	T	C		0.243	2.029	0.044
	C	T		0.095	2.766	0.006

[a]Estimated haplotype frequency.
[b]Monte-Carlo p-value from 10^4 replications.
Note: p-values of global score statistics based on 10^4 replications were 0.047 for UCP2-UCP3 haplotypes, 0.0028 for UCP3 haplotypes.
doi:10.1371/journal.pone.0029650.t004

Mutazioni del mtDNA possono modificare la longevità delle cellule
Aplotipo CAC <
Aplotipo TGT >

Nessun vento è favorevole
per chi non sa dove andare, ma
per noi che sappiamo,
anche la brezza sarà preziosa.
Rainer Maria Rilke